Environmental Health Engineering and Management Journal 2019, 6(3), 203–213
http://ehemj.com
doi 10.15171/EHEM.2019.23

Environmental Health Engineering and Management Journal

Original Article

Environmental Health Engineering and Management

Open Access Publish Free

Removal of Acid Orange 7 dye from aqueous solutions using polyaniline-modified rice bran: isotherms, kinetics, and thermodynamics

Marzieh Bagheri*, Esmail Mardani

Department of Chemical Engineering, Jami Institute of Technology, Isfahan, Iran

Abstract

Background: Today, due to increasing usage of dyes in various industrials and their destructive effects on health and environment, it is necessary to remove them from industrial wastes. Although there are few studies on the use of rice bran modified with polyaniline (RB/PANI) for removal of different dyes, but the effect of this adsorbent on the removal of Acid Orange 7 (AO7) dye has not been evaluated yet. Therefore, this study was conducted to investigate the removal of AO7 dye by RB/PANI as an adsorbent.

Methods: The adsorbent characteristics were determined using scanning electron microscopy (SEM) and Fourier transform infrared (FT-IR) spectroscopy. Also, the adsorbent surface area was measured by Brunauer–Emmett–Teller (BET) technique. The method of one-factor-at-a-time was used to optimize various factors including pH, temperature, and adsorbent dosage.

Results: The optimal values for the factors affecting AO7 dye removal were calculated. It was revealed that the maximum dye removal was obtained at pH = 3, temperature = 25˚C, dye concentration = 30 mg/L, adsorbent dosage = 30 mg/L, and contact time= 60 minutes. The maximum removal percentage for RB/PANI was 97.13%. It was also revealed that Langmuir isotherm is the best fitted isotherm model.

Conclusion: According to the results, the polyaniline-modified rice bran could be used as an excellent adsorbent for the removal of AO7 from aqueous solutions. The maximum dye removal efficiency for AO7 was obtained at pH = 3. Also, it was revealed that AO7 dye removal follows the pseudo-second-order kinetic model and it is a spontaneous process.

Keywords: Temperature, Adsorption, Coloring agents, Kinetics, Thermodynamics

Citation: Bagheri M, Mardani E. Removal of Acid Orange 7 dye from aqueous solutions using polyaniline-modified rice bran: isotherms, kinetics, and thermodynamics. Environmental Health Engineering and Management Journal 2019; 6(3): 203–213. doi: 10.15171/EHEM.2019.23.

Article History:
Received: 10 April 2019
Accepted: 24 June 2019
ePublished: 9 August 2019

***Correspondence to:**
Marzieh Bagheri
Email: miss.bagheri40@yahoo.com

Introduction

Contamination of water resources by various contaminants has always been a critical global environmental issue. Among various contaminants of water, dyes in many views are considered as the most dangerous contaminants (1). Synthetic dyes are widely used in various industries such as textile, leather, food, hygienic-cosmetics, printing, paper, plastic, and pigment production (2,3). In textile factories, for example, large volumes of water are used through dying phases. Considering the fact that dye is never perfectly fixed on textiles, the wastewater produced by these industries usually contains high amounts of dye (4). Studies show that 700 to 1000 million tons of various dyes are annually synthesized in countries around the world, of which almost 10% to 15% entering the environment without going through any treatment (5). In addition, 70% of the total dyes producing in the world belong to the family of Azo dyes, which are highly stable and non-biodegradable in nature environments, and also have toxic, mutative, and carcinogenic effects due to their nitrogen double bond and aromatic rings (6,7). Some of these dyes are not only toxic, but also threaten aquatic life and its biological systems. Even low concentrations of dyes can reduce water clarity, so they can affect photosynthetic and photochemical activities through impeding the light penetration into the water. On this basis, it seems crucially necessary to find an effective and cost-effective solution for the removal of contaminants and recycling of water (8). Several methods have been proposed for removal of dye from aqueous solutions, which can be divided into three categories of physical (9), chemical (10), and biological (11). Among the physiochemical solutions, the process of adsorption is considered as an effective and cost-effective method for removal of dye from wastewater produced by textile industries (12). The main benefits of this method include simple design, simple control,

suitable speed, high efficiency, and cost-effectiveness (13). Recently, several studies have been conducted on using inexpensive adsorbents produced from agricultural wastes such as stick powder (14), corn stems (15), and garlic skin (16), peanut hull (17), and rice bran (18). Due to their special chemical structures, these materials are able to absorb cationic materials such as heavy metals and cationic dyes, and their surfaces can be chemically modified, so they can be applied for the absorption of anionic dyes as well. One of these modifiers is polyaniline, which is an aromatic amine with unique properties such as being easily protonated, being perfectly stable, being doped rapidly and easily, having extensive spreading ability, being economic, having several factor groups on the surface, and recyclability (19,20).

Polyaniline has an extensive active surface, and since it is insoluble in aqueous solutions, it can be easily separated from these solutions. Therefore, the formerly mentioned conducting polymer of Polyaniline has been widely used for the removal of contaminants present in water. However, it is worth mentioning that due to the insolubility of polyaniline in aqueous solutions, it is not able to remove the contaminants on its own surface, hence, in many studies, polyaniline has been used as the modifier of the surfaces of adsorbents (21). The present study genuinely aimed to investigate the removal efficiency of Acid Orange 7 (AO7) dye using rice bran modified with polyaniline (RB/PANI).

Materials and Methods

Reagents and Materials

The dye of AO7 ($C_6H_{11}N_2NaO_4S$ molecular formula) with a molecular weight of 350.3 g/mol was purchased from Alvan Sabet Company of Hamedan, Iran (Figure 1). Aniline and ammonium persulfate were purchased from Merck Company. To adjust pH, HCl and NaOH 0.1 M were used. The unwashed rice bran was supplied by Qadir Rice Factory (Jozdan, Isfahan).

Apparatus

A single-radiation UV-Visible spectrophotometer (UV-2100PC, JENUS, China) was used to measure the absorption spectrum of samples. In this study, the concentration of AO7 dye was spectrophotometrically measured at a wave length of 478 nm (19). A digital pH-meter (Jenway 3020, UK) was used to measure pH. To separate adsorbent from the solution, the samples were centrifuged by Sigma101 at 5000 rpm. In order to mix the solutions, a magnetic stirrer (MR3001, Heidolph, Germany) was used. The morphology of RB/PANI was evaluated using a scanning electron microscopy (SEM) (XLC30, Philips, Netherland). The materials were measured using a digital scale (Extend model, Taiwan) with a precision scale of 0.001 g. The FT-IR (Tensor model, Germany) was used to detect the existence the functional groups of RB/PANI. In this study, all the experiments were repeated two times to ensure the trustworthiness of the results.

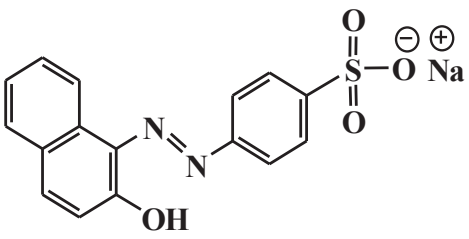

Figure 1. Structure of AO7 dye.

Analysis and Measurement

Preparation of Acid Orange 7 Solution and Calibration Curve

Firstly, a basic solution with concentration of 1000 mg/L was produced using AO7 dye. For this purpose, 1 g of the dye was poured into a 1000 M container, and then, it was brought up to the desired volume using distilled water. In addition, 5 mL of acetone was also added to the container for better dye solvation. In order to produce the solutions required for the experiments, the basic solution was diluted. In order to calculate the maximum wavelength, 10 mg/L of AO7 dye was put in a UV-Vis spectrophotometer. The adsorption of the dye was reported at the wavelength of 300 to 700 nm. The results also showed that the maximum absorption of the dye was at the wavelength of 494 nm, accordingly, the calibration curve of the dye was drawn, which was equal to $R^2 = 0.9989$. The percentage of dye removal by the rice bran modified with Polyaniline was calculated using Eq. (1).

$$\text{Decolourization}(\%) = \frac{A_0 - A}{A_0} \times 100 \quad (1)$$

Where A_0 denotes the initial adsorption value of the dye solution in the absence of the adsorbent and A denotes the dye solution final adsorption value after adding the adsorbent.

Preparation of adsorbent

To remove the possible contamination from the purchased rice bran, 100 g of rice bran was washed with 0.1 M nitric acid solution three times. Afterwards, it was again washed with distilled water a few times so that the pH of the solution under the filter paper was adjusted with the pH of distilled water. Then, 10 g of the prepared rice bran and 4 g of aniline were poured into a container. Afterwards, 250 mL of 1.0 M HCl as the polar solvent was added to the mixture, and then, the mixture was stirred for at least 30 minutes using a stirrer. In another container, 15 g of ammonium persulfate was added to 250 mL of 1.0 M HCl. Once the content of the first container was stirred for at least 30 minutes, the contents of the second container were poured into the first container, and the container was put on the stirrer for another 2 hours until the completion of the reaction. Afterwards, the stirred final solution

was poured onto a filter paper and washed with distilled water until the pH of the solution in the container under the filter paper was equalized with the pH of distilled water. Ultimately, the resulting paste was put close to a dehumidifier in a desiccator for 24 hours until it was completely dried (22).

pH effect on the dye removal process

The most effective parameter on the removal of dye is pH, which not only affects the surface load of the adsorbent, but also affects the ionization of the materials present in the solution, and factor groups on the active sites of the adsorbent as well. In order to investigate the effect of pH on dye removal, six containers (100 mL) containing 100 mL of 30 mg/L AO7 solution were prepared. The solutions pH were adjusted to 2-10 through adding suitable amounts of 0.1 M HCl and NaOH. It is worth mentioning that for both adsorbents (rice bran and RB/PANI), the fixed dosage of 30 mg/L was selected. The solutions were put on a magnetic stirrer for 60 minutes at temperature of 25˚C. For better separation, a centrifuge device was used in all experiments. At the end, the solutions were filtered with a filter paper. The absorption of solutions was measured using the UV-Vis spectrophotometer at a wave length of 494 nm, and then, compared with the initial absorbance before adding the adsorbents.

Effect of dye concentration on removal process

Dye concentration is another effective factor in dye removal by the adsorption. In order to reach an optimal initial concentration, the experiments performed in the previous steps were performed again under similar conditions, but with altered dye solution concentrations. In this regard, 100 mL of AO7 dye solution with various concentrations of 5, 10, 15, 20, 25, 30, 35, 40, and 45 mg/L was prepared with adsorbent dosage of 30 mg/L, fixed stirrer speed, temperature of 25˚C, and pH of 3 and contact time= 60 minutes.

Effect of adsorbent dosage on dye removal process

In order to determine the optimal adsorbent dosage, 100 mL of the dye solution with the optimal concentration of 30 mg/L with respectively 10, 20, 30, 40, and 50 mg/L of each adsorbent was poured into containers separately. The condition for all solutions was pH = 3, temperature = 25˚C, contact time = 60 minutes, and the stirrer speed remained constant.

Effect of contact time on dye removal process

In order to investigate the effect of contact time on the dye removal performance of the adsorbents at temperature = 25˚C, AO7 dye solutions with initial concentration of 30 mg/L and pH of 3 were prepared in 100 mL samples. To each sample, 30 mg/L of the adsorbent was added and the solutions were afterwards put on a magnetic stirrer at a fixed speed for 15, 30, 45, 80, 100, and 120 minutes, respectively.

Effect of temperature on dye removal process

To study the effect of temperature on the adsorption process in the desired samples, samples were provided under similar conditions to the previous sections (pH = 3, adsorbent dosage = 30 mg/L, and initial concentration of dye = 30 mg/L) and put on the stirrer at temperatures of 30, 35, 45, 50, 60, 70, and 80˚C for 60 minutes.

Adsorption Isotherms: Adsorption isotherm is a curve that expresses the variation in the amount of material adsorbed by the adsorbent at a constant temperature. In order to express the relationship between adsorption and the concentration of the dye remaining in the solution, various different models are usually used, among which the models of Langmuir, Freundlich, Temkin, D-R, and Generalized were used in the present study (23).

Langmuir Isotherm Model: The Langmuir adsorption isotherm model includes single-layer adsorption, assuming that bio-adsorption takes place monotonously. Based on this adsorption energy model, when the adsorbent surface is all unified, the molecules of the adsorbate will not be able to move on the surface of the adsorbent. The Langmuir equation is expressed in Eq. (2):

$$\frac{C_e}{(x/m)} = \frac{1}{ab} + \frac{1}{a} C_e \quad (2)$$

where C_e denotes the concentration of the adsorbate in a balance mode, parameters a and b are the Langmuir adsorption constants, and x/m is the amount of adsorbed dye per weight of the adsorbent (24).

Freundlich Isotherm Model: This model expresses adsorption in a heterogeneous surface in terms of adsorption energy, and is expressed as the Eq. (3).

$$\log q_e = \log K_f + \frac{1}{n} \log(C_e) \quad (3)$$

where K_f and n are Freundlich constants, $\log K_f$ denotes y-intercept, $1/n$ is the slope of Freundlich curve, and q_e denotes the adsorption capacity in a balance mode. This model is best applicable to low densities (25).

Temkin Isotherm Model: This model is used to estimate the effects of indirect interactions between the adsorbent and adsorbate in the process of adsorption. It is worth mentioning that this isotherm is only applicable to a medium range of ion concentration. The Temkin isotherm equation is expressed as Eq. (4).

$$q_e = B_1 \ln(K_T) + B_1 \ln(C_e) \quad (4)$$

where K_T is the equation constant (L/mg). The constants of K_T and B_1 can be calculated through drawing the q_e curve according to $\ln(C_e)$ (26).

D-R Isotherm Model: In this model, the mechanism of adsorption is described through distribution of Gaussian energy for heterogeneous surfaces. Similar to Temkin

model, this model is only applicable to a medium range of ion concentration. The D-R isotherm is presented in Eq. (5) (27).

$$\ln(q_e) = \ln(q_{max}) - B\varepsilon^2 \quad (5)$$

where q_{max} denotes maximum adsorption capacity (mg/g) and ε is the D-R constant and is obtained through Eq. (6).

$$\varepsilon = \left[RT\ln\left(1+\frac{1}{C_e}\right)\right]^2 \quad (6)$$

where R is the ideal gas constant (8.314 J/mol.K) and T denotes temperature (K).

Generalize Isotherm Model: This model is expressed by Eq. (7).

$$\ln\left[\left(\frac{q_{max}}{q_e}\right)-1\right] = \ln(K_G) - N\ln(C_e) \quad (7)$$

where K_G denotes the saturation constant (mg/L), N denotes the group connection constant, q_{max} denotes the maximum adsorbent adsorption (mg/g), C_e and q_e denote the balanced concentration of dye in solution and adsorbent, respectively. K_G and N can be obtained through drawing the diagram of $\ln\left[\left(\frac{q_{max}}{q_e}\right)-1\right]$ based on $\ln(C_e)$ and finding its y-intercept and slope (28).

In the present study, the above-mentioned isotherm models were used to evaluate and analyze the data obtained from the experiments. The parameters obtained from different models provide important information about the mechanism of bio-adsorption, the properties of the surface, and the adsorption willingness of the adsorbent. Linear regression is usually applied to determine the best adsorption isotherm while the applicability of the adsorption equation is determined through calculating the coefficients of the equation.

Adsorption kinetics

The kinetics of adsorption sheds light on the chemical and physical properties of adsorbent and the adsorbate particles, and also reveals the influence of adsorption mechanism. In order to determine the mechanism of adsorption process, several parameters including chemical reactions, penetration control, and mass transmission are usually investigated in multiple kinetics models under various laboratory conditions. In the present study, however, the four models of pseudo-first-order, pseudo-second-order, intramolecular penetration, and Elovich model were used.

Pseudo-First-Order equation

The pseudo-first-order equation is usually used to determine the speed of the adsorption of a material dissolved in a solution It is expressed as Eq. (8).

$$\ln(q_e - q_t) = \ln q_{eq} - K_1 t \quad (8)$$

Where q_e and q_t denote the amount of AO7 dye adsorbed during a balance mode and at time of t(min), respectively, and K_1 is the constant of adsorption speed (min^{-1}), supposing that the variable is linear, K_1 can be calculated through drawing ln (q_e – q_t) curve according to t (29).

Pseudo-Second-Order equation

In pseudo-second order equation, it is assumed that the process of adsorption can be controlled through chemical absorption. The pseudo-second-order equation is expressed as Eq. (9).

$$\frac{t}{q_t} = \frac{1}{K_2 q_e^2} + \frac{1}{q_e}t \quad (9)$$

If the equation follows the pseudo-second-order, the diagram of t/q_t must be linear against t. K_2 is the constant of speed in the pseudo-second-order equation, which is calculated by t/q_t against t (30).

The kinetic model of intramolecular penetration

The intramolecular penetration model is expressed through Eq. (10). In this model various adsorption phases it can be referred to transferring of the adsorbate molecules from solution phase to the surface of the adsorbent particles, and the transferring of these molecules to the inside of the pores of the solid surface.

$$q_t = K_{id}t^{1/2} + c \quad (10)$$

By drawing q_t based on $t^{1/2}$, the reaction speed constant of intramolecular penetration model of (K_{id}) can be determined based on the curve slope ($min^{1/2}$ mg/g) (31).

The Elovich kinetics model

The Elovich model was initially developed for chemical absorption of gas by solid phases, however, it was later applied to adsorption of material from solution phases as well. This model is described according to Eq. (11), where β denotes the surface coverage (g/mg) and α denotes the initial adsorption speed (mg/g.min). By drawing q_t according to Lnt, the values of α and β can be obtained through the curve slope and y-intercept (31).

Thermodynamics study

By performing thermodynamics studies, one can find out whether a process is endothermic, exothermic, spontaneous, or nonspontaneous. The most important parameters that would be studied in this section would be enthalpy changes (ΔH), changes in Gibbs free energy (ΔG°), and entropy changes (ΔS). In order to perform thermodynamic calculations, first, the constant of apparent valance of adsorption (K_d) will be expressed through Eq. (11).

$$K_d = \frac{q_e}{C_e} \quad (11)$$

Where q_e denotes the amount of AO7 removed by the adsorbent in the moment of balance and C_e denotes the balanced concentration of dye in the solution (mg/L). Changes in Gibbs free energy (ΔG°) show the level of spontaneity and it is calculated through Eq. (12).

$$\Delta G^\circ = -RT\ln K_d \quad (12)$$

Where R denotes the ideal gas constant, which is equal to 8.314 J/mol.K, and T denotes absolute temperature (K). And yet the most important thermodynamic values such as ΔG°, ΔH°, and ΔS° are related to each other through Eq. (13).

$$\Delta G^\circ = \Delta H^\circ - T\Delta S^\circ \quad (13)$$

The equations (12-14) show that thermodynamic values are easy to obtain.

$$\ln K_d = \frac{\Delta S}{R} - \frac{\Delta H}{R} \quad (14)$$

By drawing the linear curve of $\ln K_d$ based on 1/T, a straight line would be resulted whose y-intercept represents entropy changes and its slope gives represents enthalpy changes (32).

Results

Characteristics of adsorbent

The SEM was used to characterize surface morphology of RB/PANI before AO7 dye adsorption (Figure 2). Also, BET test was used to measure the surface area of dried powders. BET test was taken from RB/PANI and the results are summarized in Table 1. In addition, FTIR spectra were selected to study the functional groups of rice bran (Figure 3a) and RB/PANI (Figure 3b).

The effect of pH on dye removal by rice bran and RB/PANI are illustrated in Figure 4. As shown in this figure, pH 3 is the best condition for AO7 dye removal using rice bran and RB/PANI.

The influence of AO7 dye concentration on the dye removal by RB/PANI as the adsorbent is demonstrated in Figure 5a. Based on the results, the AO7 dye removal sharply decreased when the concentration of AO7 dye increased between 30 and 45 ppm. The effect of adsorbent dosage on the dye removal is shown in Figure 5b. As shown in this figure, increasing the amount of the adsorbents between 10 and 20 mg/L was effective in increasing AO7 dye removal. However, adding more than 30 mg/L of the adsorbent did not have a significant effect on AO7 dye removal.

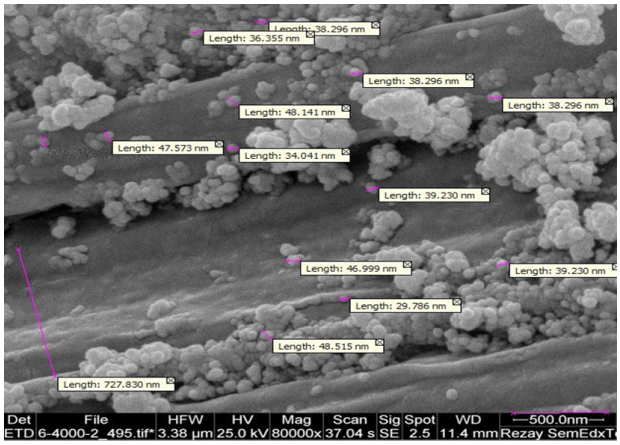

Figure 2. SEM image of rice bran modified with polyaniline (RB/PANI).

Table 1. Pore characteristics of pure rice bran modified with polyaniline (RB/PANI)

Adsorbent	Total pore volume (cm^3/g)	Mean pore diameter (nm)	Special surface area (m^2/g)
Rice bran modified with polyaniline	0.3415	50.678	26.955

The effects of contact time and temperature on AO7 dye removal by RB/PANI are presented in Figures 6a and 6b. As shown in these figures, both contact time and temperature had significant effect on RB/PANI dye removal efficiency.

In this study, the equilibrium adsorption data of AO7 dye onto RB/PANI were analyzed using 5 isotherm models including Langmuir, Freundlich, Dubinin-Radushkevich (D-R), and Generalized isotherms (Figure 7) (Table 2). The best fitted isotherm was introduced based on the values of the R^2 in the linear regression plot.

In the present study, four models of pseudo-first-order, pseudo-second-order, intra-molecular penetration, and Elovich were used to investigate the removal of AO7 dye by the polyaniline-modified rice bran (Table 3). As shown in Figure 8, the adsorption of the AO7 dye by polyaniline-modified rice bran follows the pseudo-second-order kinetic model.

Thermodynamic parameters for AO7 dye removal by RB/PANI are summarized in Table 4, and the plot of $\ln K_d$ versus 1/T is shown in Figure 9.

Discussion

The SEM image captured from RB/PANI shows that the adsorbent particles have a heterogeneous non-crystalline structure and also have so many pores that facilitate the process of adsorption. Similar recent studies have proven that heterogeneous structures increase contact surface, and result in higher adsorption of organic compounds. As shown in Figure 2, the particles of polyaniline are distributed on the rice bran in a heterogeneous and lumpy state, indicating that the adsorbent has a lot of exchange sites on its surface. In addition, the presence of particles smaller than 50 nm were shown in Figure 2. Based on the BET test, some characteristics such as the specific surface area, total pore volume, and mean pore diameter were calculated (Table 1). In the FT-IR spectrum of the polyaniline-modified rice bran, the peak at 3405 cm^{-1}

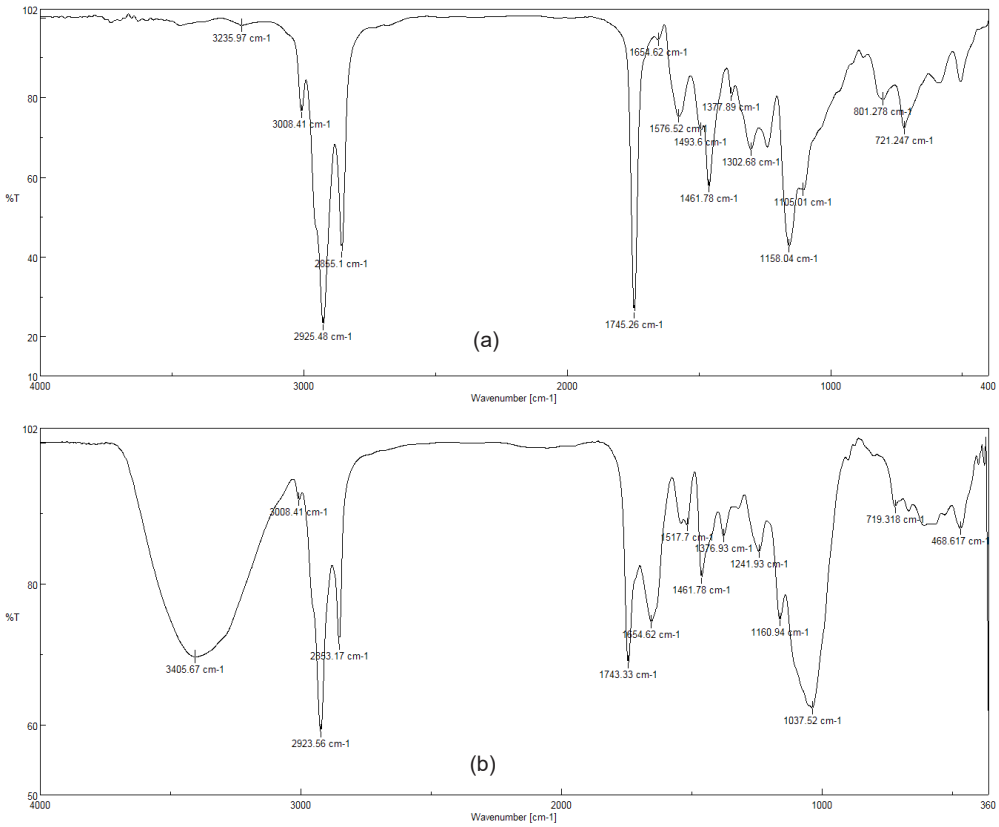

Figure 3. (**a**) FT-IR spectra of rice bran. (**b**) FT-IR spectra of rice bran modified with polyaniline (RB/PANI).

area is associated with tensile vibrations of N-H group in the structural unit of polyaniline, which can be a sign that polyaniline is connected to rice bran. The presence of polyaniline in rice bran led to minor changes in FT-IR spectrum, which can be due to the overlap of its index peak and rice bran peak. The peak at 1150 cm^{-1} area of the N-C gradient vibrations and the adsorption bar at 2923 cm^{-1} area show the tensile vibrations of the H-C aliphatic (CH_3) sp^3 (Figure 3b).

According to Figure 4, when pH is reduced, the adsorption efficiency improves and vice versa. In this regard, the most suitable pH was found to be equal to 3. This is due to the change in the ionization of factor groups existing in the adsorption sites, which results in change in the adsorbent surface load and ionization of materials existing in the

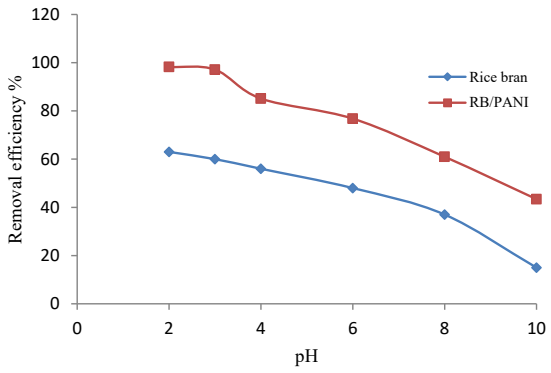

Figure 4. The effect of pH on removal of AO7 dye by RB/PANI.

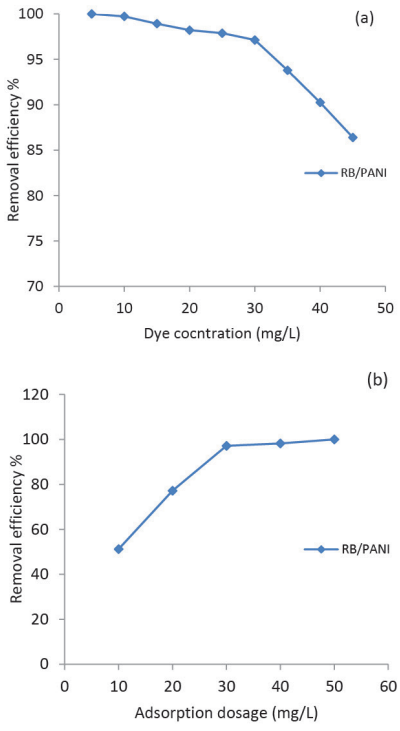

Figure 5. (a) The effect of AO7 dye concentration and (b) the effect of adsorbent dosage on the dye removal.

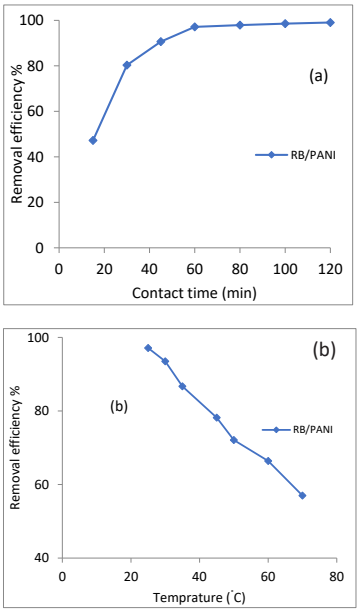

Figure 6. (a) The effect of contact time and (b) the effect of temperature on the dye removal.

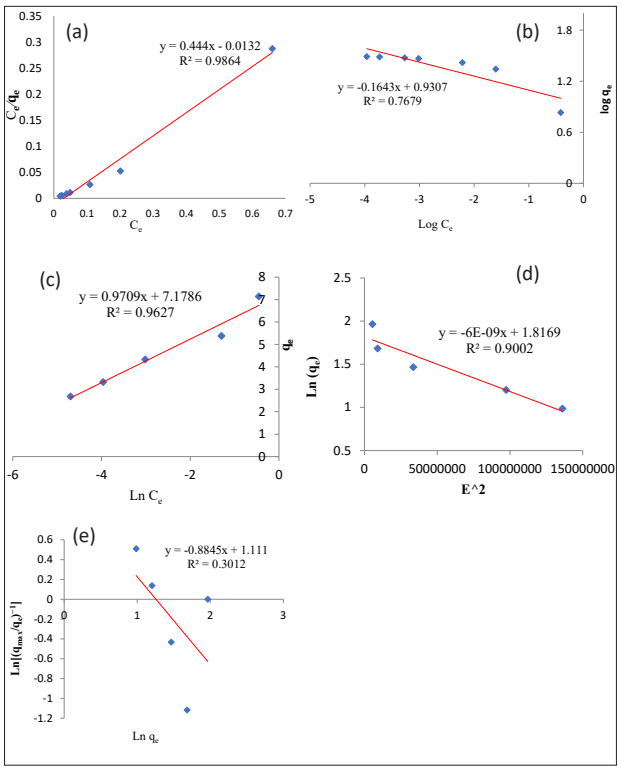

Figure 7. The results of fitting for (a) Langmuir, (b) Freundlich, (c) Temkin, (d) D-R, and (e) generalized isotherms.

Table 2. Langmuir, Freundlich, Temkin, Dubinin-Radushkevich (D-R), and Generalized isotherms constants for the adsorption of AO7 dye by RB/PANI

Langmuir Isotherm			
q_{max} (mg/g)	**K_L (L/mg)**	**R_L**	**R^2**
4.4333	3920.5751	0.000937	0.9864
Temkin Isotherm			
K_T (L/mg)	**B**		**R^2**
0.9709	7.1786		0.9627
Generalized Isotherm			
N	**K_G**		**R^2**
-0.8845	3.0374		0.3012
Freundlich Isotherm			
1/n	**n**		**K_f (mg/g)**
-6.086	-0.1643		2.5363
Dubinin-Radushkevich Isotherm			
q_e (mg/g)	**B**		**R^2**
5.203	$-9E^{-12}$		0.6521

solution as well. In other words, in the present study, when the pH was reduced, the amount of H^+ present in the environment increased, which lead to the transference of the NH_2 factor group on the adsorbent surface into NH_3^+, therefore, the willingness of the So_3^- factor group existing in the AO7 dye to adsorb was increased. At alkaline pH levels, the concentration of hydroxyl ions in the solution increases. These hydroxyl ions compete against dye ions for active adsorption sites in order to become the adsorbent, and therefore, reduce the efficiency (33). According to Figure 5a, the dye concentration of 30 mg/L is selected as the best concentration under the mentioned conditions. The results showed that at lower concentrations, for example, at 10 mg/L, dye removal was almost 100%. But as the concentration of dye increases, the concentration of 10 mg/L will no longer be sufficient, because every adsorbent has limited number of active sites which will be saturated at high dye concentrations. In this case, the surface of the adsorbent will no longer be able to adsorb, and as a result, the dye removal percentage decreases (34). In addition, Figure 5b shows that the maximum dye removal of 97.13% is obtainable through applying 30 mg/L of the adsorbent. However, the results showed that with increase of adsorbent dosage, dye adsorption also increases. Therefore, it can be concluded that the increased removal efficiency through increased adsorbent dosage is due to the increased number of active sites on the adsorbate, and therefore, higher levels of AO7 dye adsorption by the adsorbent as the adsorbent dosage is increased and more active sites are provided. In addition, since the concentration of dye is also limited, once the number of active sites exceeds the amount of dye, many of the sites will remain free (35). It was also revealed that during the initial 30 minutes, a decline in dye concentration was observed, which was followed by increased adsorption rate. This is due to the diversity of active sites on the external surfaces of the adsorbent at the onset of the process of adsorption.

Next, by prolonging the time from 30 minutes to 60 minutes, the process of adsorption continued but with a

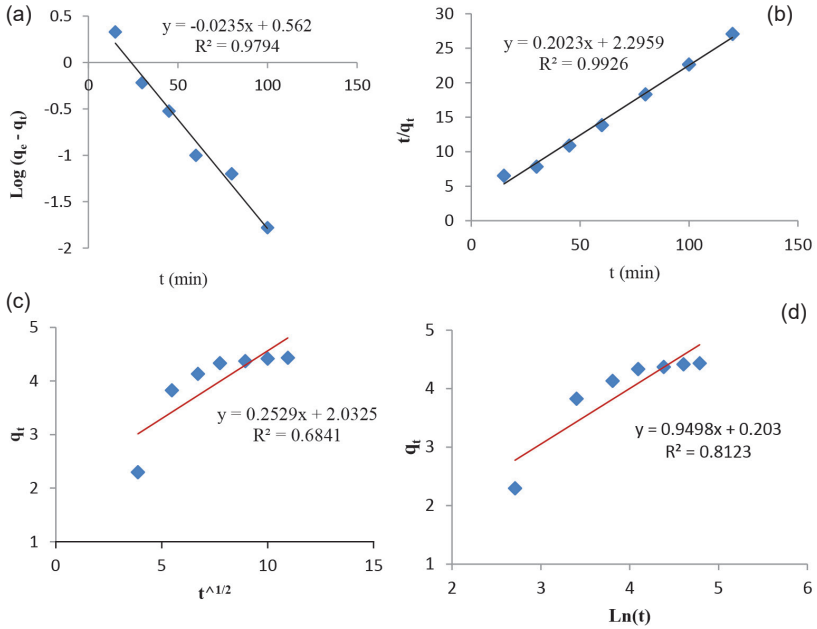

Figure 8. The results of fitting of (a) pseudo-First-order, (b) pseudo-second-order, (c) intra-particle diffusion, and (d) Elovich kinetic models.

Table 3. Parameters of Pseudo-first-order, Pseudo-second-order, Intra-particle diffusion, and Elovich kinetic models for the adsorption of AO7 dye by RB/PANI

Pseudo-First-Order Equation Model				
LSE	**$q_{e\,(exp)}$**	**$q_{e\,(cal)}$**	**K_2 (min^{-1})**	**R^2**
1.0937	4.4333	1.7542	0.05412	0.9794
Pseudo-Second-Order Equation Model				
LSE	**$q_{e\,(exp)}$**	**$q_{e\,(cal)}$**	**K_2 (min^{-1})**	**R^2**
0.1927	4.4333	4.9232	0.0178	0.9926
Intra-particle Diffusion Model		**Elovich Kinetic Model**		
K_{id} ($min^{1/2}$ mg/g)	**R^2**	**α (mg/g.min)**	**β (g/mg)**	**R^2**
0.2529	0.6841	0.5630	4.0032	0.8323

decreased intensity compared to the initial 30 minutes. In this case, since the majority of the active sites existing on the surface of the adsorbent were occupied, the molecules of AO7 dye would have to penetrate the insides of the pores, which is usually a slower process. After 60 minutes, the amount of adsorption remained relatively constant, which is due to the reduction and or saturation of the active sites hosting the adsorbate (Figure 6a) (36). As shown in Figure 6b, with increase of temperature, dye removal by the adsorbent of RB/PANI decreases, because by increasing temperature, the adsorption forces between the surface of adsorbent and dye molecules are decreased, in addition, it must be taken into account that adsorption is an exothermic process. On the other hand, increased dye removal capacity at increased temperature may be due to the increased speed of dye molecules resulting in increased contact between AO7 dye molecules and the adsorbent surface (37). As shown in Table 2, RL is in the range of $0 < RL < 1$ for Langmuir isotherm, and it can be concluded that AO7 dye removal by RB/PANI is done well (38). In addition, the numerical value of n is less than one for Freundlich isotherm. Since, n represents the distribution of adsorbed particles attached to the surface of the adsorbent, so it can be concluded that the adsorbent surface has a heterogeneous state (39). Also, in order to determine the best model for adsorption isotherm, correlation coefficient was used in the present study. The correlation coefficients of five isotherm models under study (Figure 7) shows that the Langmuir isotherm, with a correlation coefficient of 0.9864 is the most suitable model for the adsorption of AO7 using RB/PANI adsorbent. Since the Langmuir isotherm is only valid for the adsorption of adsorbate in aqueous solutions by bio-adsorbents with limited number of unified sites in a single layer, it can be concluded that AO7 dye is adsorbed by RB/PANI in a single layer and relatively monotonous state (40). Based on the results of Table 3, there is a significant difference between the equilibrium adsorption capacity ($q_{e\,(exp)}$) and calculated equilibrium adsorption capacity ($q_{e\,(cal)}$) for pseudo-first-order model. This difference led to an increase in the least squares error (LSE) in this model, while, there was no significant difference between the two

Table 4. Thermodynamic parameters for AO7 dye removal by RB/PANI

T(K)	ΔH(kJ/mol)	Δs(KJ/K.mol)	ΔG(KJ/mol)
298	-25.142	84.603	-25186.548

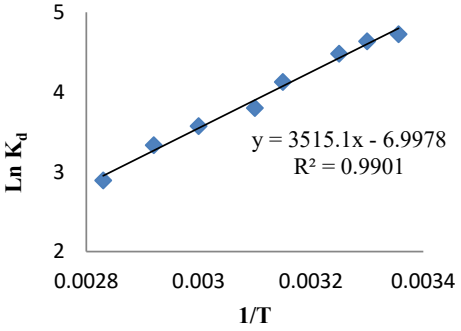

Figure 9. Plot of the adsorption of AO7 dye onto RB/PANI.

parameters [($q_{e\,(exp)}$) and ($q_{e\,(cal)}$)] for pseudo-second-order model. By taking into account the R^2 values obtained from the diagrams of pseudo-first-order, pseudo-second-order, intramolecular penetration, and Elovich models, it can be inferred that removal of AO7 dye follows the pseudo-second-order kinetics model, in addition, the R^2 value obtained for the kinetics model of pseudo-second-order was equal to 0.9926. According to Table 4, the negative enthalpy changes show that the process of adsorption of AO7 dye by RB/PANI is an exothermic process in nature. In addition, the magnitude of the enthalpy gives information on the characteristics of adsorption process including physical, chemical, and physiochemical absorption. Nevertheless, the negative values of Gibbs free energy showed that the adsorption process is spontaneous. Positive ΔS° value reflects the affinity of the pine cone for RB203 dye as well as the increase in randomness at solid-solution interface during dye adsorption (41).

Conclusion

The present study investigated the removal process of AO7 dye by Polyaniline-modified rice bran. In this study, the factors affecting the process of dye removal were investigated and the optimal value or state for each factor was determined. Among five isotherm models studied, Langmuir isotherm model was the best fitted model. In addition, it was revealed that the process of adsorption follows the kinetic model of pseudo-second-order.

In addition, thermodynamic studies showed that the process of adsorption of AO7 dye by RB/PANI is an exothermic one and is also spontaneous. According to the results, Polyaniline-modified rice bran can be a perfect adsorbent for removal of AO7 dye from aqueous solutions.

Acknowledgements

The authors would like to appreciate Jami Institute of Technology for its logistic support, which led to the completion of this dissertation.

Ethical issues

Authors are aware of, and comply with, best practice in publication ethics, specifically with regard to authorship (avoidance of guest authorship), dual submission, manipulation of Figures, competing interests, and compliance with policies on research ethics. Authors certify that submitted work is original and no data from the study has been or will be published elsewhere separately.

Competing interests

The authors declare that there is no conflict of interests.

Authors' contributions

All authors were equally participated in all aspects of this study like data collection, data analyses, and manuscript writing.

References

1. Fegousse A, El Gaidoumi A, Miyah Y, El Mountassir R, Lahrichi A. Pineapple bark performance in dyes adsorption: optimization by the central composite design. J Chem 2019; 2019: 3017163. doi: 10.1155/2019/3017163.
2. Kim SP, Choi MY, Choi HC. Characterization and photocatalytic performance of SnO2–CNT nanocomposites. Appl Surf Sci 2015; 375(part A): 302-8. doi: 10.1016/j.apsusc.2015.09.044.
3. Miyah Y, Lahrichi A, Idrissi M, Khalil A, Zerrouq F. Adsorption of methylene blue dye from aqueous solutions onto walnut shells powder: equilibrium and kinetic studies. Surfaces and Interfaces 2018; 11: 74-81. doi: 10.1016/j.surfin.2018.03.006.
4. Singh S, Sidhu GK, Singh H. Removal of methylene blue dye using activated carbon prepared from biowaste precursor. Indian Chem Eng 2019; 61(1): 28-39. doi: 10.1080/00194506.2017.1408431.
5. Chen KC, Wu JY, Yang WB, Hwang SC. Evaluation of effective diffusion coefficient and intrinsic kinetic parameters on azo dye biodegradation using PVA-immobilized cell beads. Biotechnol Bioeng 2003; 83(7): 821-32. doi: 10.1002/bit.10730.
6. Latif S, Rehman R, Imran M, Iqbal S, Kanwal A, Mitu L. Removal of acidic dyes from aqueous media using *Citrullus lanatus* peels: an agrowaste-based adsorbent for environmental safety. J Chem 2019; 2019: 6704953. doi: 10.1155/2019/6704953.
7. Mahmoodi NM, Arami M. Numerical finite volume modeling of dye decolorization using immobilized titania nanophotocatalysis. Chem Eng J 2009; 146(2): 189-93. doi: 10.1016/j.cej.2008.05.036.
8. Zahran SA, Ali-Tammam M, Hashem AM, Aziz RK, Ali AE. Azoreductase activity of dye-decolorizing bacteria isolated from the human gut microbiota.

Sci Rep 2019; 9(1): 5508. doi: 10.1038/s41598-019-41894-8.
9. Inyinbor AA, Adekola FA, Olatunji GA. Adsorption of rhodamine B dye from aqueous solution on *Irvingia gabonensis* biomass: kinetics and thermodynamics studies. S Afr J Chem 2015; 68: 115-25. doi: 10.17159/0379-4350/2015/v68a17.
10. Sarker R, Chowdhury M, Deb AK. Reduction of color intensity from textile dye wastewater using microorganisms: a review. International Journal of Current Microbiology and Applied Sciences 2019; 8(2): 3407-15. doi: 10.20546/ijcmas.2019.802.397.
11. Baddouh A, Amaterz E, El Ibrahimi B, Rguitti MM, Errami M, Tkach V, et al. Enhanced electrochemical degradation of a basic dye with Ti/Ru0.3Ti0.7O2 anode using flow-cell. Desalin Water Treat 2019; 139: 352-9 doi: 10.5004/dwt.2019.23274.
12. Ansari R, Hossainzadeh Khanesar P. Application of spent tea leaves as an efficient low cost biosorbent for removal of anionic surfactants from aqueous solutions. Eur Chem Bull 2013; 2(5): 283-9. doi: 10.17628/ecb.2013.2.283-289.
13. Bhatnagar A, Sillanpää M. Utilization of agro-industrial and municipal waste materials as potential adsorbents for water treatment—a review. Chem Eng J 2010; 157(2-3): 277-96. doi: 10.1016/j.cej.2010.01.007.
14. Boudia R, Mimanne G, Benhabib K, Pirault-Roy L. Preparation of mesoporous activated carbon from date stones for the adsorption of Bemacid Red. Water Sci Technol 2019; 79(7): 1357-66. doi: 10.2166/wst.2019.135.
15. Vučurović VM, Razmovski RN, Miljić UD, Puškaš VS. Removal of cationic and anionic azo dyes from aqueous solutions by adsorption on maize stem tissue. J Taiwan Inst Chem Eng 2014; 45(4): 1700-8. doi: 10.1016/j.jtice.2013.12.020.
16. Asfaram A, Fathi MR, Khodadoust S, Naraki M. Removal of Direct Red 12B by garlic peel as a cheap adsorbent: kinetics, thermodynamic and equilibrium isotherms study of removal. Spectrochim Acta A Mol Biomol Spectrosc 2014; 127: 415-21. doi: 10.1016/j.saa.2014.02.092.
17. Yang C, Gong R, Liu B, Liu H, Sun Y, Ke L. Utilization of powdered peanut hull as biosorbent for removal of anionic dyes from aqueous solution. Ying Yong Sheng Tai Xue Bao 2004; 15(11): 2195-8. doi: 10.1016/j.dyepig.2004.05.005.
18. Hong GB, Wang YK. Synthesis of low-cost adsorbent from rice bran for the removal of reactive dye based on the response surface methodology. Appl Surf Sci 2017; 423: 800-9. doi: 10.1016/j.apsusc.2017.06.264.
19. Wei J, Zhang C, Du Z, Li H, Zou W. Modification of carbon nanotubes with 4-mercaptobenzoic acid-doped polyaniline for quantum dot sensitized solar cells. J Mater Chem C 2014; 2(21): 4177-85. doi: 10.1039/C4TC00021H.
20. Kumar R, Ansari MO, Barakat MA. DBSA doped polyaniline/multi-walled carbon nanotubes composite for high efficiency removal of Cr(VI) from aqueous solution. Chem Eng J 2013; 228: 748-55. doi: 10.1016/j.cej.2013.05.024
21. Kumar R, Ansari MO, Barakat MA. Adsorption of brilliant green by surfactant doped polyaniline/MWCNTs composite: evaluation of the kinetic, thermodynamic, and isotherm. Ind Eng Chem Res 2014; 53(17): 7167-75. doi: 10.1021/ie500100d.
22. Li W, Kim D. Polyaniline/multiwall carbon nanotube nanocomposite for detecting aromatic hydrocarbon vapors. J Mate Sci 2011; 46(6): 1857-61. doi: 10.1007/s10853-010-5013-3.
23. Ayawei N, Ebelegi AN, Wankasi D. Modelling and interpretation of adsorption isotherms. J Chem 2017; 2017: 3039817. doi: 10.1155/2017/30398171.
24. Langmuir I. The constitution and fundamental properties of solids and liquids. J Franklin Inst 1917; 183(1): 102-5. doi: 10.1021/ja02268a002
25. Hameed BH, Din AT, Ahmad AL. Adsorption of methylene blue onto bamboo-based activated carbon: Kinetics and equilibrium studies. J Hazard Mater 2007; 141(3): 819-25. doi: 10.1016/j.jhazmat.2006.07.049.
26. Aharoni C, Ungarish M. Kinetics of activated chemisorption. Part 2.—Theoretical models. J Chem Soc Faraday Trans 1977; 73: 456-64. doi: 10.1039/F19777300456.
27. Rahman N, Abedin Z, Hossain MA. Rapid degradation of azo dyes using nano-scale zero valent iron. Am J Environ Sci 2014; 10(2): 157-63. doi: 10.3844/ajessp.2014.157.163.
28. Çelebi O, Üzüm Ç, Shahwan T, Erten HN. A radiotracer study of the adsorption behavior of aqueous Ba2+ ions on nanoparticles of zero-valent iron. J Hazard Mater 2007; 148(3): 761-7. doi: 10.1016/j.jhazmat.2007.06.122.
29. Ho YS, Chiu WT, Wang CC. Regression analysis for the sorption isotherms of basic dyes on sugarcane dust. Bioresour Technol 2005; 96(11): 1285-91. doi: 10.1016/j.biortech.2004.10.021.
30. Ho YS, McKay G. Pseudo-second order model for sorption processes. Process Biochem 1999; 34(5): 451-65. doi: 10.1016/S0032-9592(98)00112-5.
31. Plazinski W, Rudzinski W, Plazinska A. Theoretical models of sorption kinetics including a surface reaction mechanism: a review. Adv Colloid Interface Sci 2009; 152(1-2): 2-13. doi: 10.1016/j.cis.2009.07.009.
32. Sartape AS, Mandhare AM, Jadhav VV, Raut PD, Anuse MA, Kolekar SS. Removal of malachite green dye from aqueous solution with adsorption technique using *Limonia acidissima* (wood apple) shell as low cost adsorbent. Arab J Chem 2017; 10(Suppl 2): S3229-38. doi: 10.1016/j.arabjc.2013.12.019.

33. Crini G, Badot P-M. Application of chitosan, a natural aminopolysaccharide, for dye removal from aqueous solutions by adsorption processes using batch studies: a review of recent literature. Prog Polym Sci 2008; 33(4): 399-447. doi: 10.1016/j.progpolymsci.2007.11.001.
34. Zarei M, Salari D, Niaei A, Khataee A. Peroxi-coagulation degradation of C.I. Basic Yellow 2 based on carbon-PTFE and carbon nanotube-PTFE electrodes as cathode. Electrochim Acta 2009; 54(26): 6651-60. doi: 10.1016/j.electacta.2009.06.060.
35. Wang S, Zhu ZH. Characterisation and environmental application of an Australian natural zeolite for basic dye removal from aqueous solution. J Hazard Mater 2006; 136(3): 946-52. doi: 10.1016/j.jhazmat.2006.01.038.
36. Senthilkumaar S, Varadarajan PR, Porkodi K, Subbhuraam CV. Adsorption of methylene blue onto jute fiber carbon: kinetics and equilibrium studies. J Colloid Interface Sci 2005; 284(1): 78-82. doi: 10.1016/j.jcis.2004.09.027.
37. Kavak D. Removal of boron from aqueous solutions by batch adsorption on calcined alunite using experimental design. J Hazard Mater 2009; 163(1): 308-14. doi: 10.1016/j.jhazmat.2008.06.093.
38. Ong ST, Lee CK, Zainal Z. Removal of basic and reactive dyes using ethylenediamine modified rice hull. Bioresour Technol 2007; 98(15): 2792-9. doi: 10.1016/j.biortech.2006.05.011.
39. Makhado E, Pandey S, Nomngongo PN, Ramontja J. Preparation and characterization of xanthan gum-cl-poly(acrylic acid)/o-MWCNTs hydrogel nanocomposite as highly effective re-usable adsorbent for removal of methylene blue from aqueous solutions. J Colloid Interface Sci 2018; 513: 700-14. doi: 10.1016/j.jcis.2017.11.060.
40. Zarei M, Pezhhanfar S, Ahmadi Someh A. Removal of acid red 88 from wastewater by adsorption on agrobased waste material. A case study of Iranian golden Sesamum indicum hull. Environmental Health Engineering and Management Journal 2017; 4(4): 195-201. doi: 10.15171/ehem.2017.27.
41. Ashraf MW, Abulibdeh N, Salam A. Adsorption studies of textile dye (chrysoidine) from aqueous solutions using activated sawdust. Int J Chem Eng 2019; 2019: 9728156. doi: 10.1155/2019/9728156.